SANDIA REPORT SAND85—0064 • Unlimited Release • UC—62E
Printed March 1986

Sintering of Coarse Ceramic Particles

G. L. Messing, D. M. Kupp, J. R. Hellmann

Prepared by
Sandia National Laboratories
Albuquerque, New Mexico 87185 and Livermore, California 94550
for the United States Department of Energy
under Contract DE-AC04-76DP00789

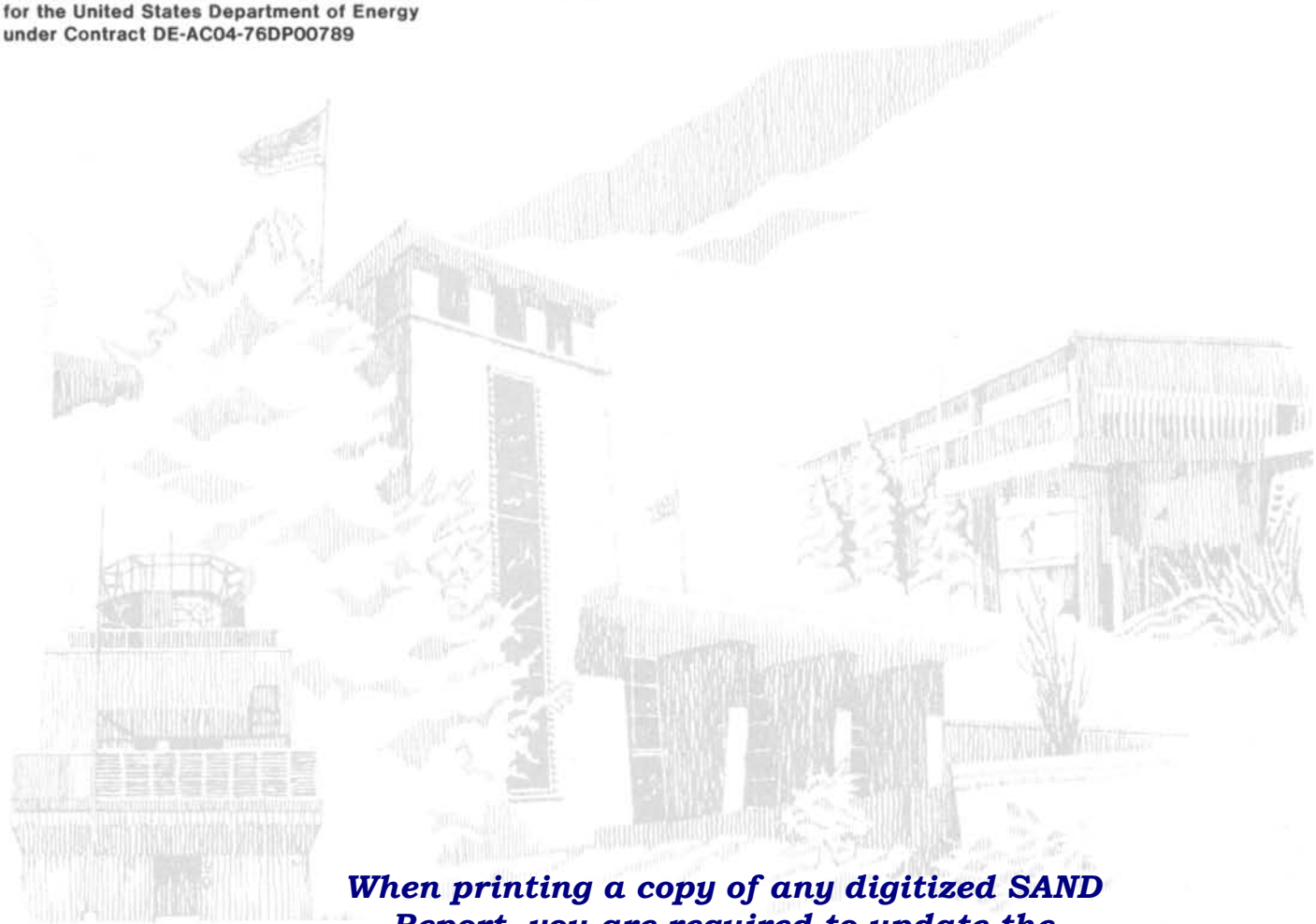

Issued by Sandia National Laboratories, operated for the United States Department of Energy by Sandia Corporation.

Printed in the United States of America
Available from
National Technical Information Service
U.S. Department of Commerce
5285 Port Royal Road
Springfield, VA 22161

NTIS price codes
Printed copy: A04
Microfiche copy: A01

SINTERING OF COARSE CERAMIC PARTICLES

March 13, 1986

G. L. Messing and D. M. Kupp
Ceramic Science Section
Department of Materials Science and Engineering
Pennsylvania State University
University Park, PA 16802

and

J. R. Hellmann
Electronic Ceramics Division, 1842
Sandia National Laboratories
Albuquerque, NM 87185

SOLAR THERMAL TECHNOLOGY
FOREWORD

The research and development described in this document was conducted within the U. S. Department of Energy's (DOE) Solar Thermal Technology Program. The goal of the Solar Thermal Technology Program is to advance the engineering and scientific understanding of solar thermal technology, and to establish the technology base from which private industry can develop solar thermal power production options for introduction into the competitive energy market.

Solar thermal technology concentrates solar radiation by means of tracking mirrors or lenses onto a receiver where the solar energy is absorbed as heat and converted into electricity or incorporated into products as process heat. The two primary solar thermal technologies, central receivers and distributed receivers, employ various point and line-focus optics to concentrate sunlight. Current central receiver systems use fields of heliostats (two-axis tracking mirrors) to focus the sun's radiant energy onto a single tower-mounted receiver. Parabolic dishes up to 17 meters in diameter track the sun in two axes and use mirrors or Fresnel lenses to focus radiant energy onto a receiver. Troughs and bowls are line-focus tracking reflectors that concentrate sunlight onto receiver tubes along their focal lines. Concentrating collector modules can be used alone or in a multi-module system. The concentrated radiant energy absorbed by the solar thermal receiver is transported to the conversion process by a circulating working fluid. Receiver temperatures range from 100°C in low-temperature troughs to over 1500°C in dish and central receiver systems.

The Solar Thermal Technology Program is directing efforts to advance and improve promising system concepts through the research and development of solar thermal materials, components, and subsystems, and the testing and performance evaluation of subsystems and systems. These efforts are carried out through the technical direction of DOE and its network of national laboratories who work with private industry. Together they have established a comprehensive, goal directed program to improve performance and provide technically proven options for eventual incorporation into the Nation's energy supply.

To be successful in contributing to an adequate national energy supply at reasonable cost, solar thermal energy must eventually be economically competitive with a variety of other energy sources. Components and system-level performance targets have been developed as quantitative program goals. The performance targets are used in planning research and development activities, measuring progress, assessing alternative technology options, and making optimal component developments. These targets will be pursued vigorously to insure a successful program.

This report describes the evaluation of several ceramic materials for application as thermal transfer media in a solid particle solar receiver. The study identified three materials (zircon ($ZrSiO_4$), silica (SiO_2), and alumina (Al_2O_3)) which are sufficiently refractory to resist aggregation and sintering under anticipated receiver storage conditions. Aggregation and sintering must be avoided to retain particle flow characteristics during numerous heating and storage cycles. Further work is necessary to develop materials with the requisite optical properties to permit heating to higher temperatures in a solar beam.

ABSTRACT

The primary objective of this program was to select a particulate ceramic for use as a thermal transfer medium in a solid particle solar receiver. The first year of the program involved an initial assessment of ceramic materials that met minimum criteria for the proposed solid particle receiver, including (1) availability in commercial quantities (i.e. tons), (2) a particle size of 100 micrometers, (3) a high melting temperature and (4) high particle flowability and the absence of aggregation (i.e. sintering) during use. The following materials were selected by the Sandia National Laboratories, Albuquerque (SNLA) group for evaluation on the basis of these requirements and from discussions with industrial vendors: alumina (Al_2O_3), silicon carbide (SiC), rutile (TiO_2), mullite ($3Al_2O_3 \cdot 2SiO_2$), silica (SiO_2), zircon ($ZrSiO_4$), zirconia (ZrO_2) and garnet ($Ca_3Al_2Si_3O_{12}$).

Standardized packing and flow tests were employed on size-classified powders (nominally 100 μm e.s.d.*) to reduce the list of candidate materials for further study. Mullite was eliminated due to inadequate flowability. Garnet was eliminated due to its propensity toward sintering during heating to 1200°C. Rutile, silica, and zircon were selected for further study because they exhibited superior flow properties due to their well-rounded particle morphology. Alumina was selected due to its resistance to sintering at elevated temperature. Silicon carbide exhibited poor resistance to sintering above 800°C, but was included for full characterization of its useful temperature range since it possesses desirable optical properties.

*equivalent spherical diameter

Sintering of the ceramics was studied by heating a 4 cm diameter by 3 cm high powder bed in air at temperatures ranging from 800 to 1500°C for one hour. The flowability of the alumina, rutile, silica and zircon was unaffected by heating from 800 to 1100°C for 1h and 24 hrs. Silicon carbide formed a well bonded mass at 1000°C as a result of the formation of a viscous glass phase on the particle surfaces during heating. All materials formed a solid mass at 1500°C.

To simulate the effect of storage bed height on sintering of the powders, a load of 0.34 MPa (50 psi) was applied to the powder beds for 1-24h at 1000°C. The silica and zircon powders were essentially unaffected by pressure whereas the alumina powder showed no aggregation due to sintering after 12h and only light aggregation after 24h. The rutile powder did not flow after one hour of this treatment.

The major factors that affect the aggregation of the coarse-grained powders are temperature and pressure. Time at temperature is of minor significance when there is no load and is only significant for alumina powder after long durations (>12h). Because it is anticipated that the solar particle receiver will operate at approximately 1000°C and that the particles will not reside at peak temperature for more than a few hours, these studies indicate that zircon, silica and alumina may be suitable for application as thermal transfer media in a solar receiver provided their optical properties permit heating to requisite temperatures in a solar beam.

LIST OF TABLES

LIST OF FIGURES

TABLE OF CONTENTS

INTRODUCTION

In July 1982, representatives of the Solar Components Division, 8453, at Sandia National Laboratories, Livermore (SNLL) requested assistance from the Ceramics Development Division, 1845 (SNLA) in the selection and evaluation of ceramic materials to be used as solar transfer media in a high temperature solar receiver. In response to that request, Division 1845 evaluated the response of selected commercially available ceramic media to ranges of temperature, pressure, and time that simulated projected storage conditions in the proposed solar receiver. Responses studied included sinterability, thermal shock resistance, and impact resistance. Division 1845 opted to contract out some of these studies and to act as an intermediary for the dissemination and interpretation of the results for Division 8453. This report documents the results of the study of the relative propensity toward sintering exhibited by several candidate ceramic materials. This work was performed by the Department of Materials Science and Engineering at the Pennsylvania State University.

High Temperature Solar Receiver Design Concept

The solar central receiver design concept employs a field of computer controlled heliostats (mirrors) to reflect incident solar radiation toward a receiver mounted on top of a tower. [1] The energy collected by the receiver is subsequently used to power a number of processes (e.g., heating gases to run turbines, production of steam, driving endothermic chemical reactions, etc.). The successful implementation of any solar receiver design is dependent upon the efficiency with which the solar radiation is converted into thermal energy, how that energy is transported and stored,

and finally, how efficiently the energy is transferred to the process of interest.

Many types of solar receiver systems have been designed and some offer levels of power generation up to 1000 MW_{th}*. In general, most systems employ gaseous or molten salt transport media coupled with process heat exchangers for the production of thermal energy at temperatures in excess of 500°C. More recent work has focused upon the use of liquid metals for thermal exchange and transport; these systems can operate to substantially higher temperatures (700°C). Each of these concepts has been employed to produce energy for thermally driven processes as well as for the generation of electricity.

Recently, it has become desirable to generate thermal energy at higher temperatures to satisfy the needs of processes requiring temperatures in excess of 700°C. The Solar Components Division, 8453 (SNLL), has been investigating an advanced receiver concept which utilizes solid refractory ceramic particles for direct absorption of the concentrated solar radiation and subsequent storage and transfer as high quality process heat [2,3]. This concept represents a major departure from conventional solar receiver designs in that the thermal transport medium is directly heated by the solar beam and relinquishes its energy directly to the process of interest, thereby reducing the need for costly heat exchange and transport systems. This concept is termed the High Temperature Solid Particle Central Receiver.

Early designs for the high temperature solid particle solar receiver focused upon achieving 100 MW_{th} energy generation with temperatures up to 1500°C and thermal storage capabilities sufficient for sustained operation through periods of inclement weather of up to 24 hours in duration [4].

*Thermal energy expressed in Megawatts

Calculations based on those designs indicate that optimum particle sizes for the ceramic thermal transfer medium range from 100 to 1000 μm, depending on particle density [2]. Departure from the starting particle size distribution is undesirable since it can significantly alter particle residence time in the solar beam, and, hence the amount of energy absorbed. Furthermore, the generation of fines may result in an enhanced susceptibility to particle aggregation due to sintering of the particle charge during high temperature storage. Aggregation can be expected to markedly decrease the flowability of the storage medium, an undesirable phenomenon where large quantities (up to 5×10^6 kg) [5] of material must be kept moving to achieve optimum thermal output.

Program Objectives

The purpose of this investigation was to determine the propensity toward sintering exhibited by several candidate ceramic materials under conditions of temperature, pressure, and time typical of storage in the proposed High Temperature Solid Particle Receiver. The data obtained in this study will lead to the selection or development of an appropriate material for use as a solid thermal transfer medium.

EXPERIMENTAL

Material Selection Criteria

Due to the severity of the operating and storage conditions projected for the solid thermal transfer medium, it is apparent that only highly refractory materials with excellent resistance to thermal and mechanical stress will survive repeated cycles through the receiver. Furthermore, the

materials used should be relatively inexpensive and available in tonnage quantities. The materials should exhibit a low tendency toward aggregation due to sintering or reaction with the surrounding environment (chute linings, storage walls, ambient and process atmospheres, etc.).

A market survey indicated that a wide variety of materials available from the abrasives industry met most of the requirements as thermal transfer media. The primary criterion sought in the initial selection of materials was the need for high refractoriness. In general, materials possessing melting points in excess of the upper limit of receiver operation (1500°C) were selected. In addition, the abrasives industry normally consumes these materials in large quantities, hence, availability and cost appear to be acceptable for application of these materials as thermal transfer media. The materials selected for evaluation are listed in Table 1. The materials can be divided into two categories:

1. Naturally occurring minerals (zircon, silica, garnet, and rutile) which are generally less expensive ($0.60 - $1.50/kg) and more abundant than synthetic materials. However, control of chemistry, homogeneity, and purity is widely variable.
2. Synthetic materials (alumina, silicon carbide, mullite, and stabilized zirconia) are somewhat more expensive ($2.00 - $4.00/kg) while chemistry, purity, and particle morphology are more easily controlled than for the naturally occurring materials.

The advantage of the synthetic materials is the ease with which the optical, thermal, and mechanical properties can be tailored to fill the requirements for thermal transfer media. However, the costs associated with materials development and synthesis may prove prohibitive to their application to the solar receiver concept.

Table 1: Materials Investigated

MATERIAL	TRADE NAME	VENDOR
Alumina-1	Alundum	Norton Co.
-2	White Al_2O_3	Carborundum Co.
-3	Duralum	Washington Mills Abrasive Co.
-4	Exolon WP	Exolon Co.
-5	Tabular Alumina	Kaiser Chemicals Co.
-6	Brown Alumina	General Abrasives Division, Dresser Industries, Inc
Silicon carbide-1	Crystolon	Norton Co.
-2	SiC Grain	Carborundum Co.
-3	Silcarbide	Washington Mills Abrasives Co.
-4	Carbolon	Exolon Co.
-5	Black SiC	General Abrasives Division, Dresser Industries, Inc
Silica	Granusil	Unimin Corporation
Garnet	Garnet	Continental Mineral Processing Corporation
Rutile	Rutile	Continental Mineral Processing Corporation
Zircon	Zircon	Continental Mineral Processing Corporation
Mullite	Fused Mullite	C. E. Minerals
Zirconia (CaO stabilized)	Stabilized Zirconia	Norton Co.

Material Characterization

The flowability of an assemblage of particles is largely determined by particle size, shape, and packing properties. The susceptibility of particles to aggregation via sintering is determined by their composition and particle size distribution. Initial characterization was performed to quantify the relative flowability and propensity toward sintering of each of the candidate materials in order to select a smaller group of materials for further evaluation as thermal transfer media.

1. Size Classification

As-received materials were size classified to -140, +170 mesh (nominal 100 μm particle size). This size range represents the minimum size considered for the solar receiver and the worst case from a sintering perspective.

2. Chemistry

X-ray analysis of the candidate materials was performed with CuK_{α} radiation from 20-80°2θ at 4°2θ/min to confirm the vendors' compositions. Where available, the vendors' chemical analyses are reported (Appendix). For those materials in which no chemical analysis was provided, spectrochemical analysis was performed using inductively coupled plasma atomic absorption spectroscopy.

3. Bulk Powder Physical Properties

The packing characteristics of each powder were quantified by comparing their pour and tap densities. The pour density represents the volume of a known weight of powder when poured into a container without agitation. The tap density represents the volume occupied by the same column of powder after the individual particles have "settled" due to mechanical agitation. The tap density of each powder was determined by vibrating a known weight of

powder to an apparent minimum volume. A vibrating table was used to cause "boiling" of the particles in a 10 ml. graduated cylinder. By continuously decreasing the amplitude of vibration, dense packing was achieved progressively from the bottom to the top of the cylinder. Once particle boiling had ceased throughout, minimal vibration was used until all particles ceased detectable movement. Poured and vibrated volumes were measured and the appropriate densities calculated.

Flowability tests were carried out following ASTM standard B213-77. This standard was modified by using a round funnel with a 3.8 mm orifice and 50 grams of powder. Each of three draining trials was timed with a hand held stopwatch and the average rate calculated.

Angle of repose tests were performed on the nominally 100 μm powders in the as-received state and after heat treating at 1200°C for 15 minutes. A glass funnel with a round orifice of 3.8 mm diameter was placed 76 mm above the surface onto which 20 ml of the powder was poured to form a heap. The interior angle of inclination (Figure 1) was measured with a protractor and visual observations concerning heap formation and flowability were made.

A matrix of temperature, pressure and time was investigated to evaluate their effects on the sintering of the candidate materials. Initially, the powders were heated for 1 hour at 800, 1000, 1100, 1200 and 1500°C. Flow rates were reported on the basis of volume per unit time. The effect of time on particle sintering was investigated at 1000°C for 1, 4, 8, 12, and 24 hours. A series of experiments in which a 39 kg load was applied to a particle bed 3.8 cm in diameter (equivalent to 34 MPa) and 3.4 cm in height was performed at 1000°C and 1250°C for the same times as studied in the sintering experiments. The powder flowability after heat treatment was measured as described above.

4. Particle properties

Particle densities were primarily determined by pycnometry. ASTM Standard C135-66 was followed with only minor modification.

Particle shape and appearance were observed by scanning electron microscopy after various experiments.

Results

1. Chemical analysis

The phase composition of each material was verified by X-ray diffraction. Compositions determined by spectrochemical analysis verified the vendors' analyses in the Appendix.

2. Bulk powder physical properties

The particle, pour, and tap densities are presented in Table 2. The packing efficiency of the powders, and thus their flowability can be gauged by comparing the pour and tap densities. Powders exhibiting higher flowability pack to a higher density during pouring because the individual particles move more easily past one and other. The pour to tap density ratio equals 1.0 if the particles pack into their most densely packed state during filling. Therefore, the smaller the ratio, the lower is the intrinsic flowability of the powder. It is noteworthy that only the garnet rutile and zircon particles have high pour to tap density ratios; mullite, alumina-2 and alumina-6 have low ratios, whereas the remainder of the powders range from 0.86 - 0.89.

Another measure of powder flowability is the packing density (defined as the ratio of tap density to particle density). Random packing of uniformly sized spherical particles generally yields a packing density of 0.62 - 0.65 [6]. In this study, only silica, garnet and rutile packed to

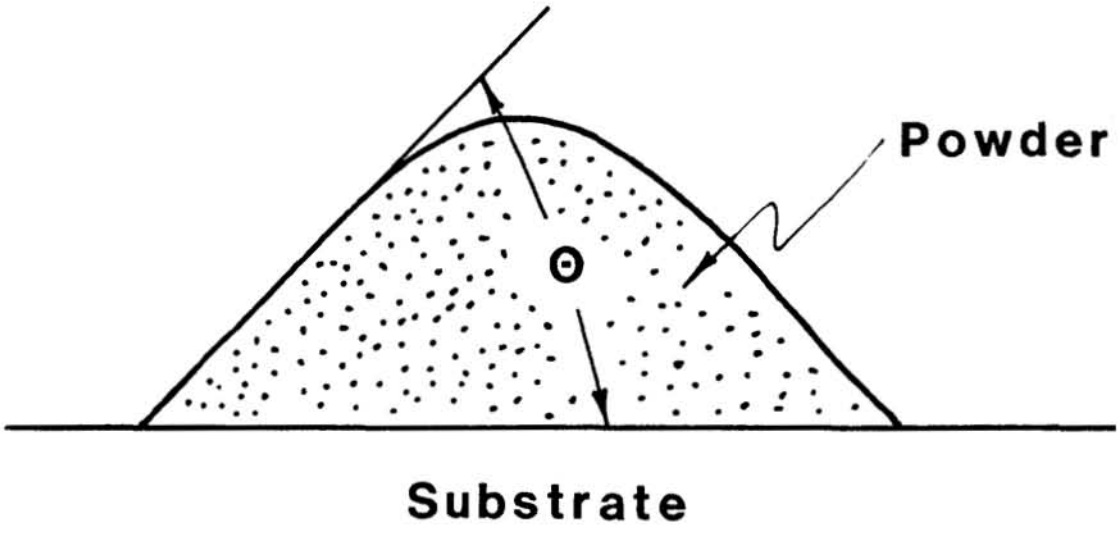

Figure 1 - Interior angle of inclination (θ) used in Angle of Repose Measurements

that level. Packing densities for the other powders ranged from 0.50 - 0.54. Such departures have previously been attributed to deviations in particle morphology and degree of aggregation from monodispersed spheres [7] and have been shown to markedly alter flowability [8].

The flowability of the powders was gauged from angle of repose tests and by noting the time for 50 grams of powder to pass through a funnel. Because the materials have different densities, a more meaningful measure is obtained by normalizing the flow rate to the particle density. These results are presented in Table 3 for the materials before and after heating at 1200°C for 15 minutes.

The angle of repose is dependent on the intrinsic flowability of the powder. The greater the angle of repose, the lower the particle flowability. After heating, those materials yielding higher flowabilities by this measure are aluminas -2, -3, and -5, and mullite. The angle of repose before and after heating varies substantially for the alumina samples. The general increase in flowability of the particles after heating suggests the flowability was hindered by moisture in the unheated powders and/or that particle rounding occurred with heating. Particle rounding was not observed during microscopic evaluation of heated particles. In most cases the angle of repose indicated improved flowability with heating, except for alumina-4 and rutile. It is noteworthy that heat treatment at 1200°C resulted in sintering of alumina-6, all silicon carbides, and garnet. Reasons for this behavior will be discussed later.

The flow rates through a small orifice can be compared on the basis of weight per unit time (ASTM Standard method) or volume per unit time. However, particle volume per unit time is a better parameter for comparing materials that differ in particle density. The volumetric flow rates were

Table 2: Bulk Powder Properties

Material	Particle Density (g/cc)	Pour Density (g/cc)	Tap Density (g/cc)	Pour/Tap Density Ratio	Packing Density Ratio
Alumina					
-1	3.96	1.83	2.07	0.88	0.53
-2	3.97	1.64	2.00	0.82	0.50
-3	3.93	1.72	1.95	0.88	0.50
-4	3.90	1.71	1.92	0.89	0.49
-5	3.81	1.75	2.04	0.86	0.54
-6	3.87	1.74	2.09	0.83	0.54
Silicon Carbide					
-1	3.19	1.52	1.71	0.89	0.54
-2	3.26	1.46	1.68	0.87	0.52
-3	3.20	1.46	1.66	0.88	0.52
-4	3.20	1.41	1.66	0.85	0.52
-5	3.09	1.45	1.68	0.86	0.54
Silica	2.65	1.53	1.71	0.89	0.64
Garnet	3.69	2.16	2.41	0.90	0.65
Rutile	4.25	2.47	2.70	0.91	0.64
Zircon	4.68	2.69	2.96	0.91	0.63
Mullite	3.05	1.16	1.51	0.77	0.50

TABLE 3: Powder Flowability

Material	Angle of Repose (as received*) (degrees)	Angle of Repose (After heating at 1200°C, 15 min.)	Flow Rate (as received*) g/sec	cc/sec	Flow Rate (After heating at 1200°C, 15 min. g/sec	cc/sec
Alumina						
-1	40	31	3.0	0.76	2.7	0.68
-2	35	25	2.4	0.60	2.6	0.65
-3	37	30	2.6	0.66	2.8	0.71
-4	25	30	2.8	0.72	2.4	0.62
-5	40	25	2.4	0.63	2.4	0.63
06	34	N.F.	3.3	0.85	N.F.	N.F.
Silicon carbide						
-1	30	N.F.	2.2	0.69	N.F.	N.F.
-2	33	N.F.	2.8	0.86	N.F.	N.F.
-3	30	N.F.	2.6	0.81	N.F.	N.F.
-4	31	N.F.	2.6	0.81	N.F.	N.F.
-5	30	N.F.	2.5	0.81	N.F.	N.F.
Silica	25	25	3.0	1.13	3.6	1.36
Garnet	29	N.F.	4.1	1.11	N.F.	N.F.
Rutile	25	30	5.0	1.18	4.8	1.13
Zircon	23	24	5.6	1.20	6.7	1.43
Mullite	35	32	N.F.	N.F.	1.5	0.49
Zirconia	40	40	5.0	0.89	5.5	0.97

N.F. = No Flow

*after size classification

calculated by dividing the mass flow rate by the particle density. When these values are compared, it is apparent that the greatest flow rates are exhibited by the natural materials: silica, rutile and zircon. Within the alumina class, alumina-1 and alumina-4 have the highest flowability in the as-received conditions. After heat treatment, alumina-3 has the highest flowability. Nevertheless, the flowability of all aluminas is still significantly less than observed for the natural materials.

Relative particle sizes and shapes can be qualitatively compared for the size fractionated powders in Figures 2-18. In general, both the alumina and silicon carbide particles possess angular shapes. The naturally occuring materials, i.e. silica, garnet, rutile and zircon, are all well rounded. The superior flowability of the naturally occurring materials can be attributed to the fact that rounded particles are less likely to bridge, occlude void space, and hinder particle flow.

CANDIDATE SELECTION

The above results were supplemented with a few additional experiments to select materials for more extensive high temperature evaluation. The rationale for materials selection is presented below.

Alumina: Alumina-6 was eliminated from further tests because it sintered when heated to 1200°C. In fact, its composition is purposely modified by Fe_2O_3 and MnO_2 additions by the manufacturer to reduce its melting temperature for production. Alumina-5 was chosen as representative of the other aluminas for further study on the basis of powder flowability and chemical composition.

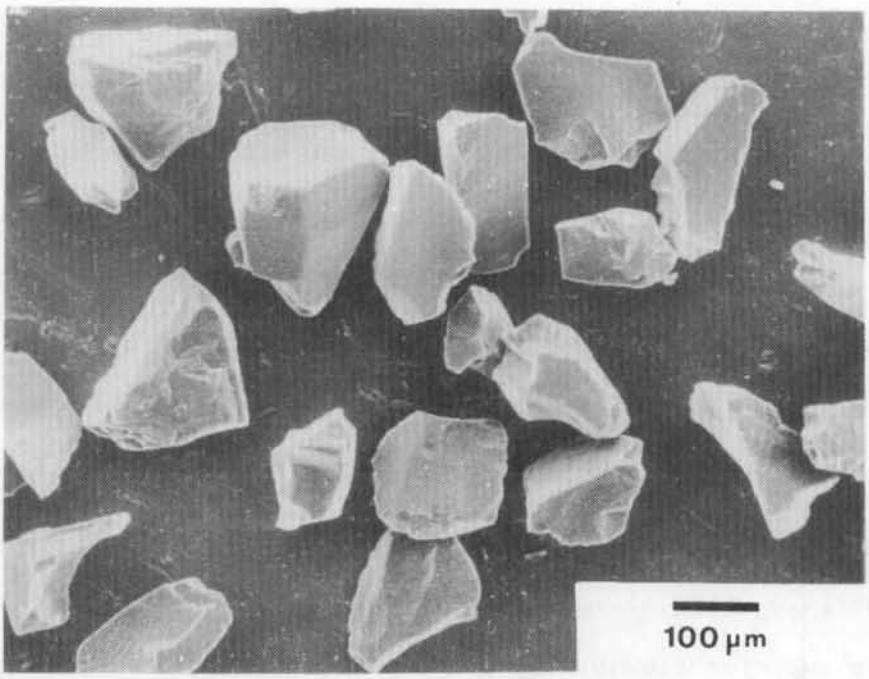

Figure 2 - Particle morphology of as-received Norton Alundum™ (alumina-1, 140/170 mesh)

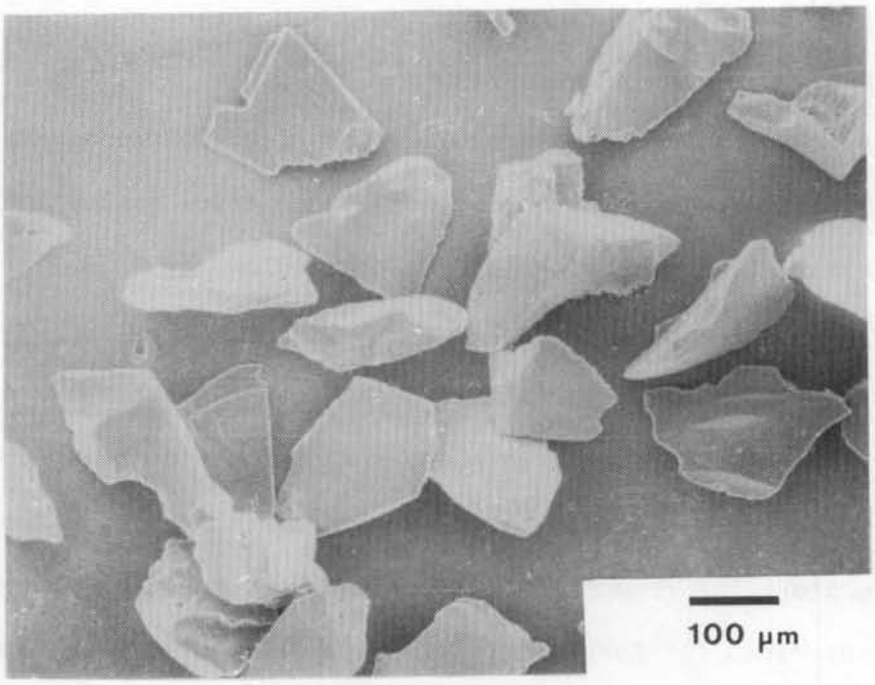

Figure 3 - Particle morphology of as-received Carborundum Co. white Al_2O_3 (alumina-2, 140/170 mesh)

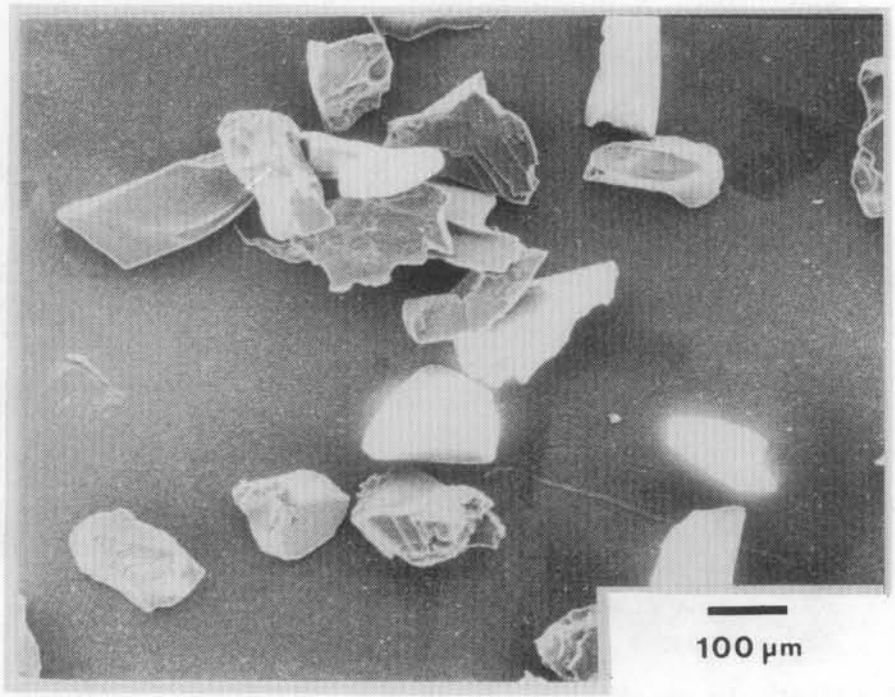

Figure 4 - Particle morphology of as-received Washington Mills Duralum™ (alumina-3, 140/170 mesh)

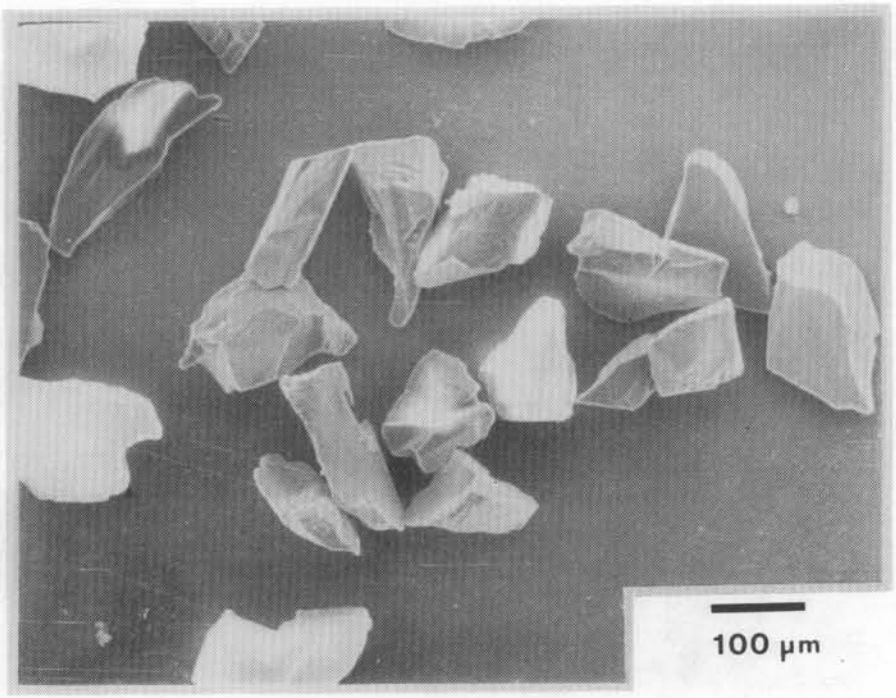

Figure 5 - Particle morphology of as-received Exolon Co. Exolon WP™ (alumina-4, 140/170 mesh)

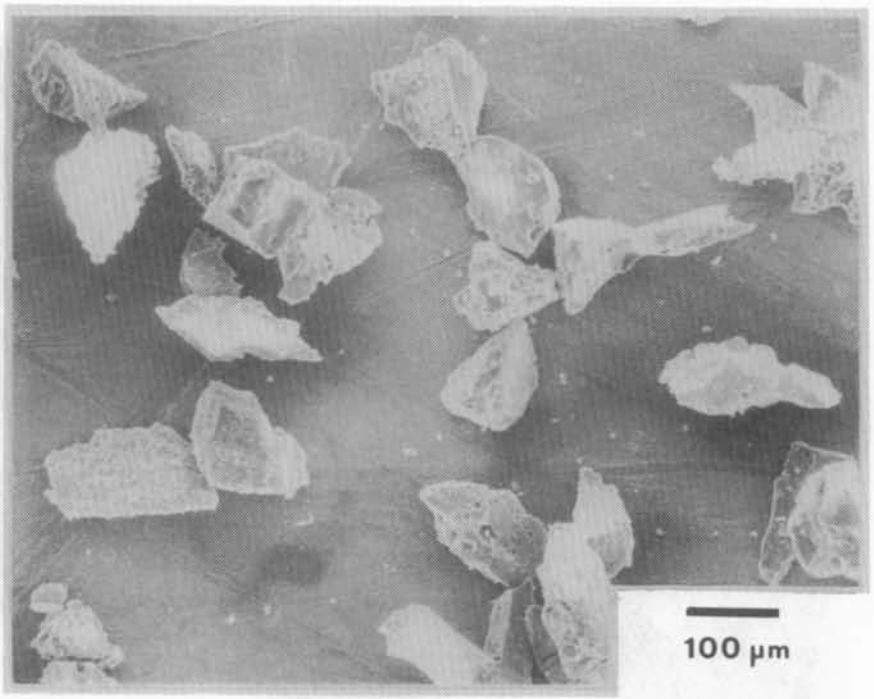

Figure 6 - Particle morphology of as-received Kaiser Chemicals tabular alumina (alumina-5, 140/170 mesh)

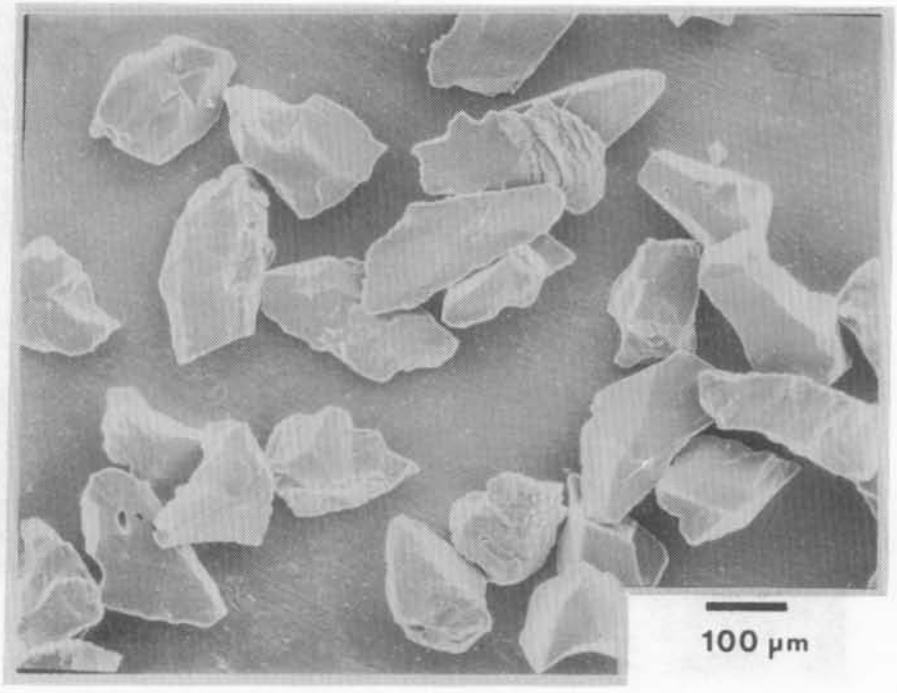

Figure 7 - Particle morphology of as-received General Abrasives brown alumina (alumina-7, 140/170 mesh)

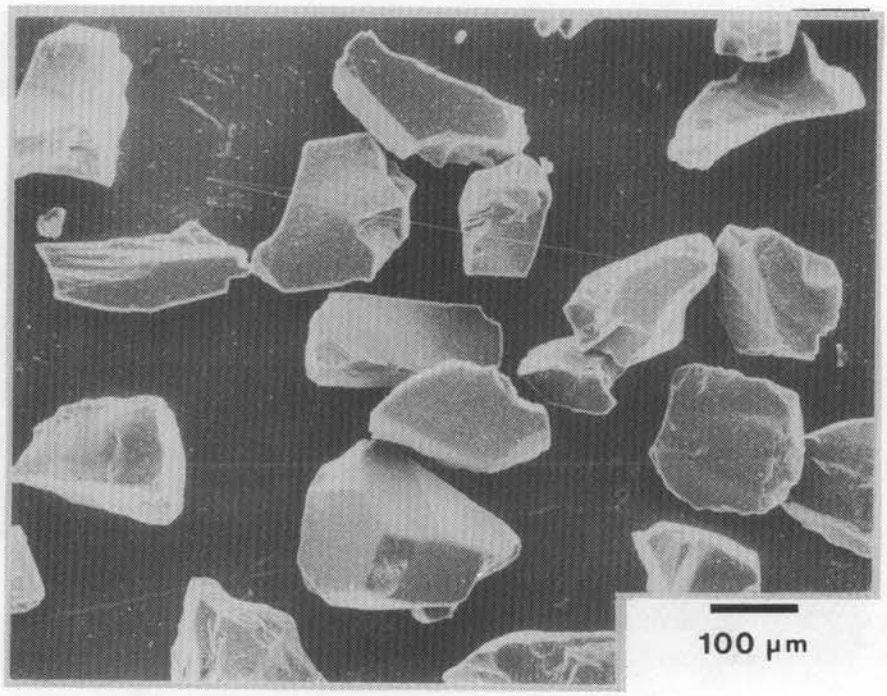

Figure 8 - Particle morphology of as-received Norton Co. Crystolon™ (silicon carbide-1, 140/170 mesh)

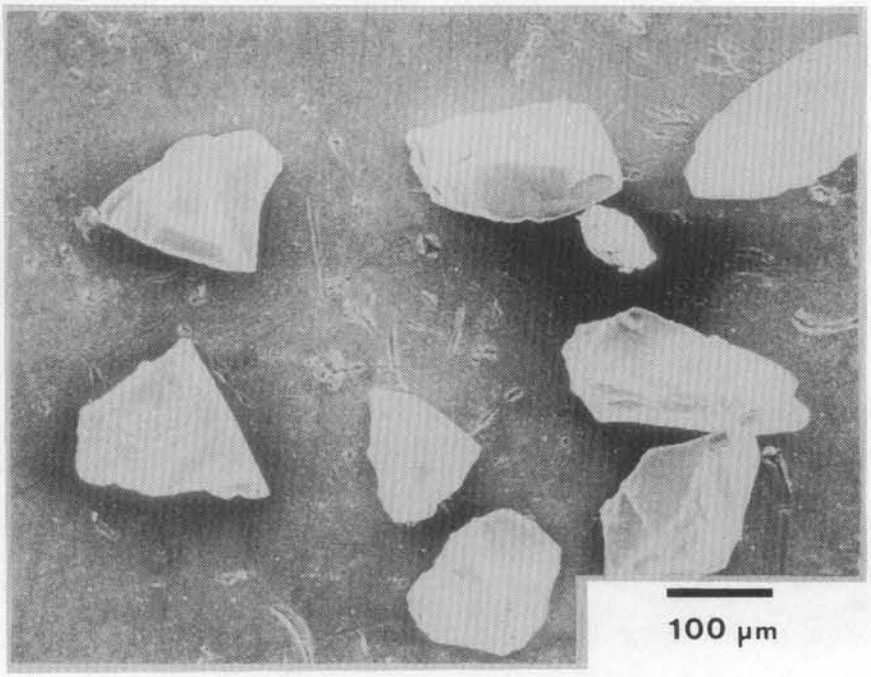

Figure 9 - Particle morphology of as-received Carborundum Co. SiC (silicon carbide-2, 140/170 mesh)

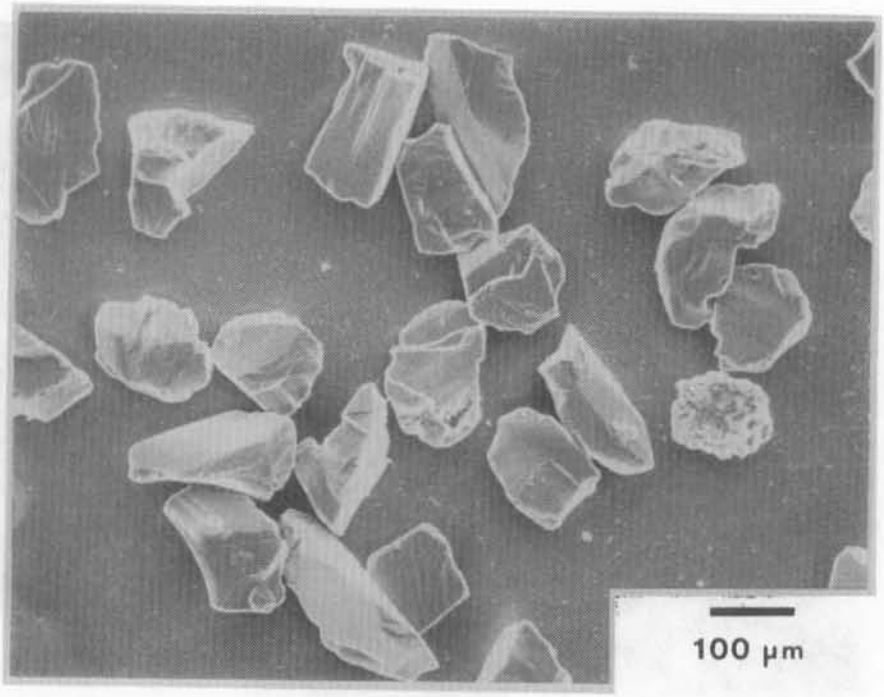

Figure 10 - Particle morphology of as-received Washington Mills Silcarbide™ (silicon carbide-3, 140/170 mesh)

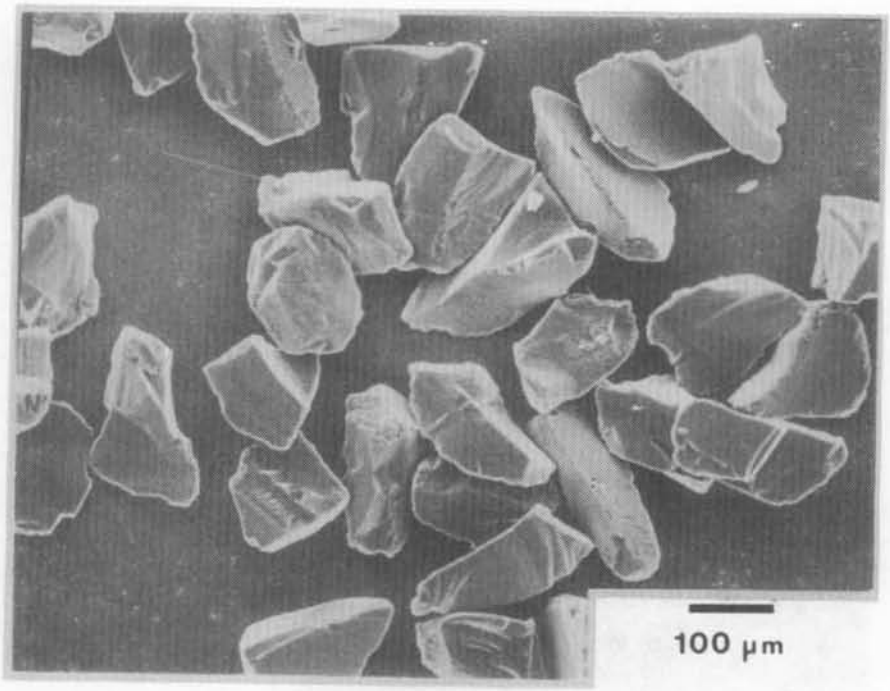

Figure 11 - Particle morphology of as-received Exolon Co. Carbolon™ (silicon carbide-4, 140/170 mesh)

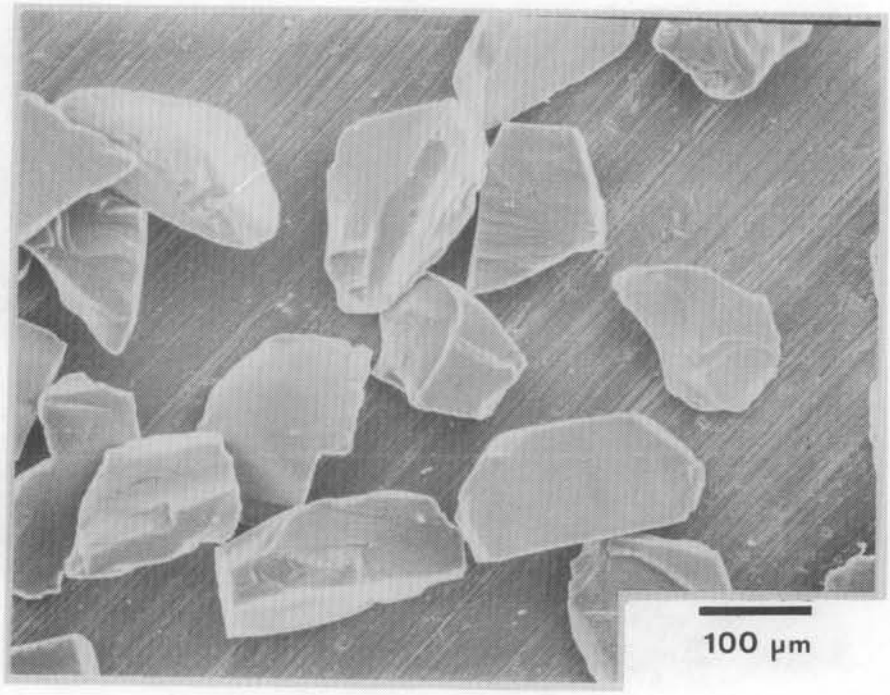

Figure 12 - Particle morphology of as-received General Abrasives black SiC (silicon carbide-5, 140/170 mesh)

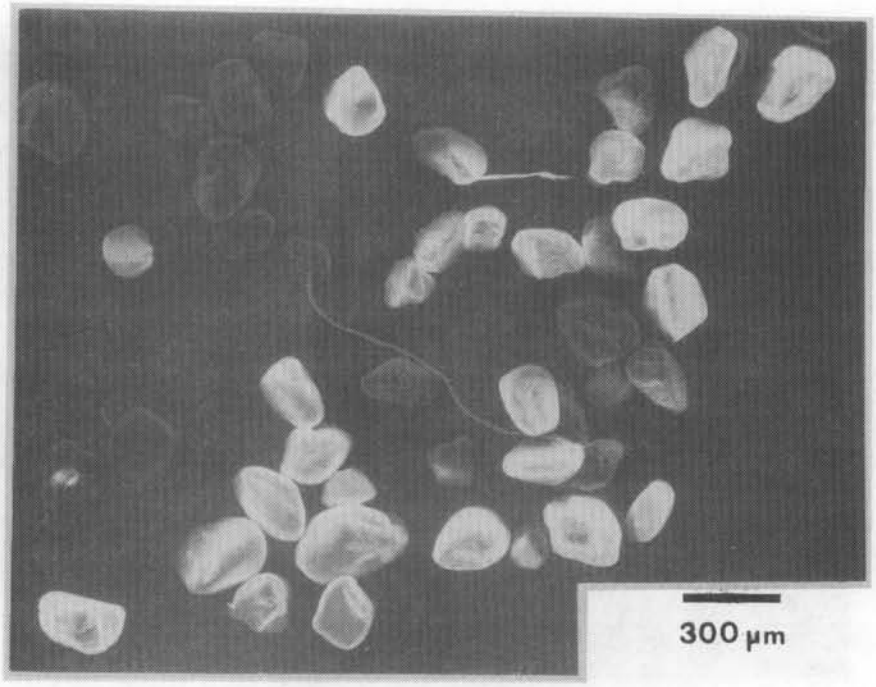

Figure 13 - Particle morphology of as-received Unimin Corp. Granusil™ (silica, 140/170 mesh)

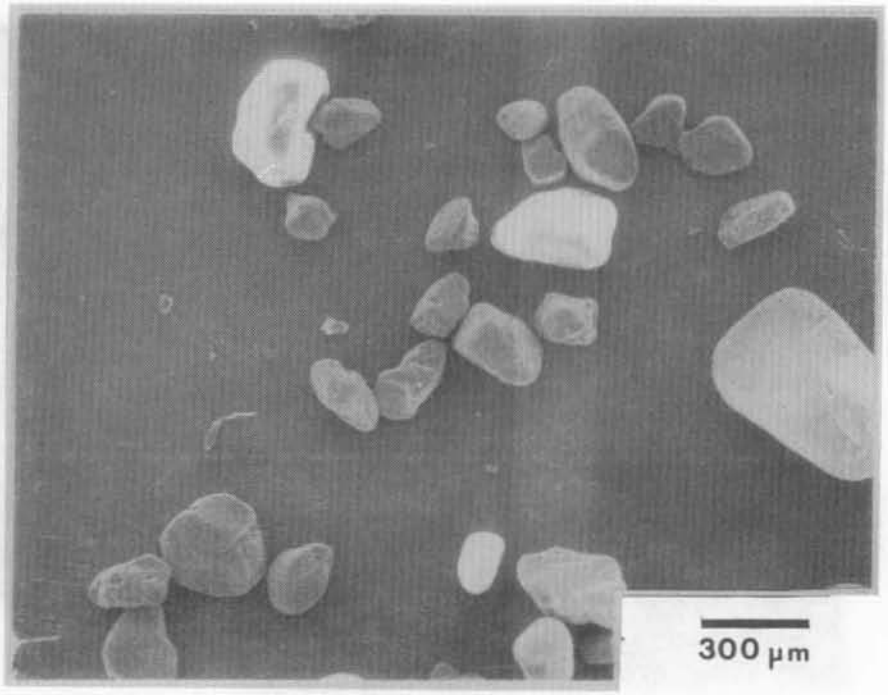

Figure 14 - Particle morphology of as-received Continental Mineral Processing Corp. Garnet (140/170 mesh)

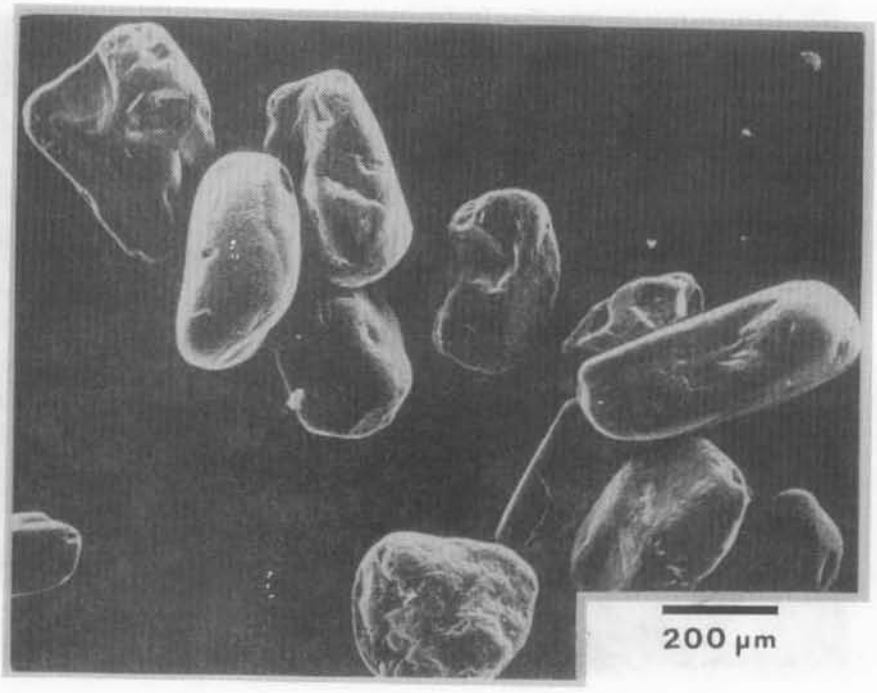

Figure 15 - Particle morphology of as-received Continental Mineral Processing Corp. TiO_2 (rutile, 140/170 mesh)

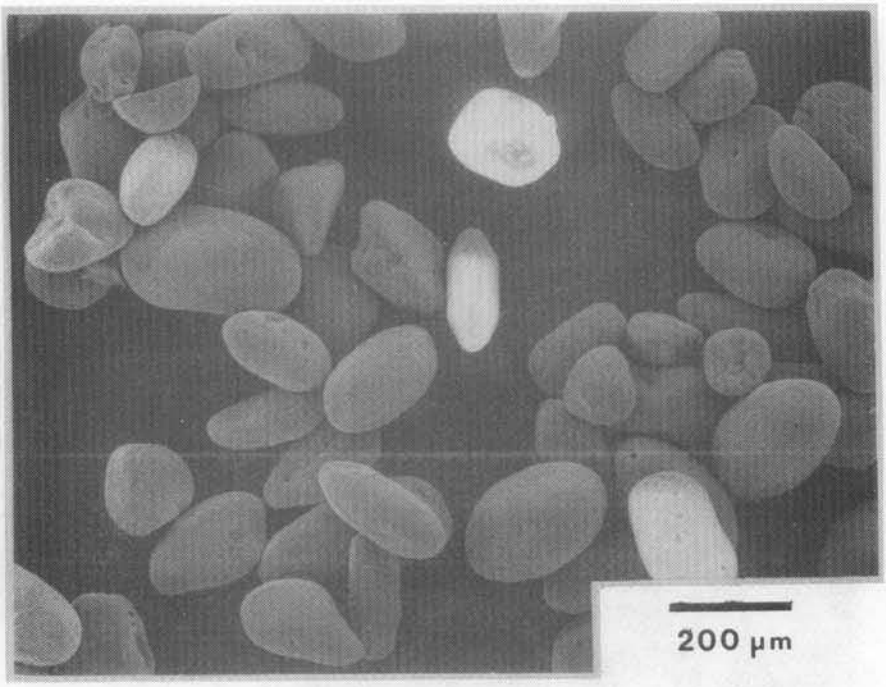

Figure 16 - Particle morphology of as-received Continental Mineral Processing Corp. $ZrSiO_4$ (Zircon, 140/170 mesh)

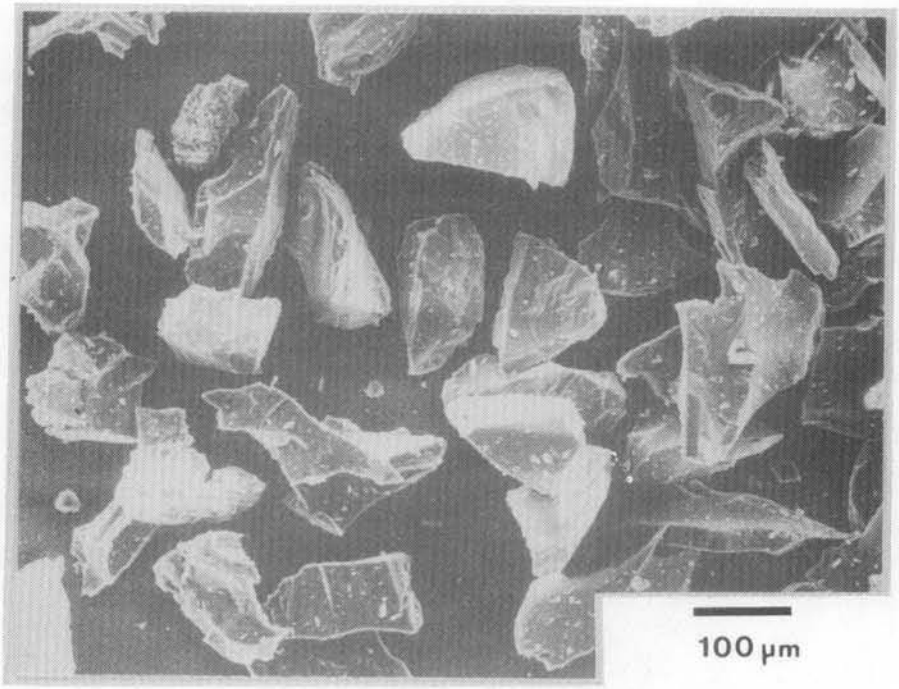

Figure 17 - Particle morphology of as-received C.E. Minerals $3Al_2O_3$ $2SiO_2$ (mullite, 140/170 mesh)

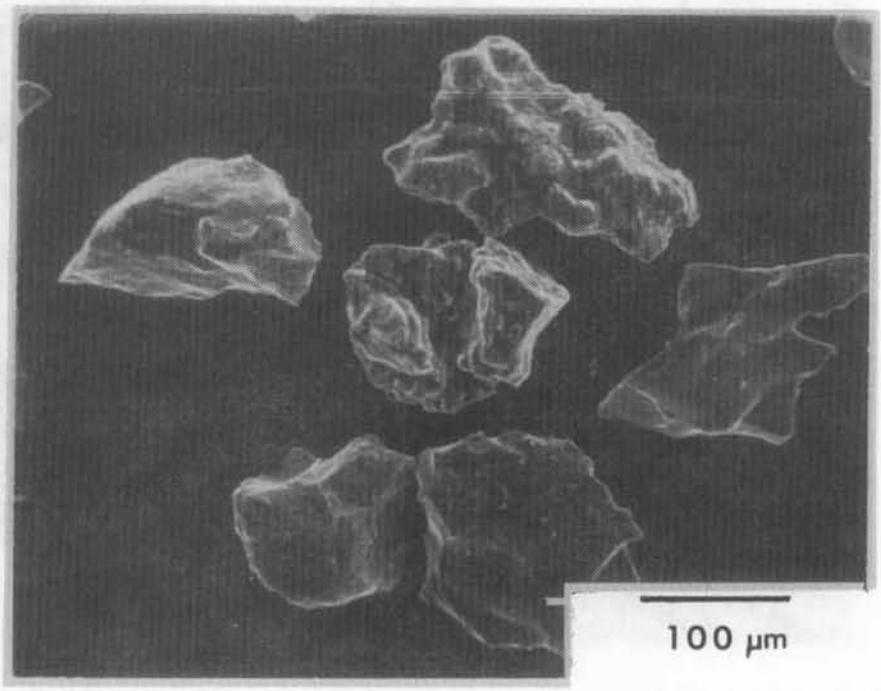

Figure 18 - Particle morphology of as-received Norton Co. partially stabilized zirconia (140/170 mesh)

Silicon carbide: All of the silicon carbides showed similar flow characteristics in the as-received condition. However, when heated to 1200°C for 15 minutes, all powders formed a coherent mass as a result of oxide formation on the silicon carbide surfaces. Because this oxide coating is liquid under these conditions, the particles bonded by a viscous sintering mechanism. Although oxidation is enhanced by the impurities present in the powder, it is believed that even a pure silicon carbide would behave similarly at 1200°C [9]. However, at the request of Division 8453 (SNLL), silicon carbide-2 was retained for further evaluation of its upper temperature limit of use since it exhibits desirable optical properties [10] and performed satisfactorily in simulated solar heating experiments [11].

Silica: The silica powder consists of rounded particles and contains 2% total impurities. Particle flow was unaffected at 1200°C because the material remains crystalline and does not melt under these conditions. Consequently, it was selected for more extensive investigation.

Garnet: The garnet powder showed excellent room temperature flowability. However, when heated to 1200°C for 15 minutes it sintered into a solid mass. Therefore, it was not considered further.

Rutile: The rutile powder was composed of well-rounded, ellipsoidal particles. Its flowability was unchanged when heated to 1200°C. Chemically, it is 96.7% TiO_2 with the major impurities being Fe_2O_3, ZrO_2, and SiO_2. Because of its dark red color and high optical absorptivity [10], it was selected for additional study.

Zircon: The zircon showed the best flowability of all the powders tested. The particles are well rounded and egg-shaped. Because its flowability remained unchanged after heating at 1200°C, it was selected for further study.

Mullite: The mullite powder did not flow at room temperature. Flowability improved, although to only half the rate of the natural materials, after heating at 1200°C. Because of its poor flowability in the as-received condition, it was not considered further.

Zirconia: The zirconia powder exhibited similar flowability compared to the aluminas. The zirconia was partially stabilized with CaO to retain the zirconia in the cubic crystal form after manufacture. Stabilization is necessary to avoid the large volume change that pure zirconia undergoes when heated. The volume change is a consequence of a martensitic phase transformation from monoclinic to tetragonal zirconia at 1170°C. The transformation is usually catastrophic in pure polycrystalline zirconia bodies. Since the as received powder consisted of a mixture of monoclinic and stabilized cubic zirconia, quenching experiments were performed to determine whether the volume change of the monoclinic ZrO_2 would have a deleterious effect on the thermal stability of the particles. The powder was quenched from 1200°C onto an alumina substrate at room temperature. Figures 18 and 19 illustrate the extent of particle fracture which occurred during the quenching experiment. Although this was a simplistic experiment, it was considered adequate to demonstrate that ZrO_2 would probably lack mechanical integrity under the repeated thermal cycling of a solar receiverand, hence, it was also eliminated from further study.

CANDIDATE MATERIALS EVALUATION

The five materials chosen for more extensive study were tested in a series of experiments in which the effects of time, temperature and applied pressure on particle aggregation were evaluated.

In the first set of tests, each of the powders was placed in a crucible with bed dimensions of 4 cm. diameter and a depth of approximately 5 cm. and

heated to temperatures from 800 to 1500°C for one hour. After cooling, the powder was removed from the crucible and the flowability was measured. When strong aggregation due to sintering occurred, the nature of the bond was examined by scanning electron microscopy.

Table 4 lists the flowability of the heated powders relative to the flowability of the as-received powder. The silicon carbide was flowable to 800°C, but formed a strongly bonded mass at 1000°C and higher. As described earlier, the bonding is a result of a viscous oxide layer that forms on the particle surfaces during heating. Figure 20 illustrates the nature of the glassy bond between particles. Although pure silicon carbide does not oxidize rapidly at 1000°C, oxidation studies of silicon carbide indicate that impurities greatly enhance oxidation kinetics [9,12]. As this powder contains free Si and Fe as impurities, it is not surprising that an extensive oxide coating was formed at 1000°C. As a result of these observations, we recommend that silicon carbide not be considered for use above 800°C.

Heating of the remaining particles to 1100°C had no adverse effect on flowability. Only zircon remained easily flowable when heated at 1200°C. After heating to 1200°C, the alumina powder could be made to flow by disturbing the particle bed with light agitation. This is because the degree of bonding was very weak relative to the bonding observed for silica, silicon carbide, and rutile. Zircon and alumina sintered after heating at 1500°C.

In the above experiments, the powders were heated for only 1 hour. Sintering and neck formation is a kinetic process in which larger necks are formed with increasing time at temperature. Aggregation due to sintering should increase with increasing time at temperature and hinder

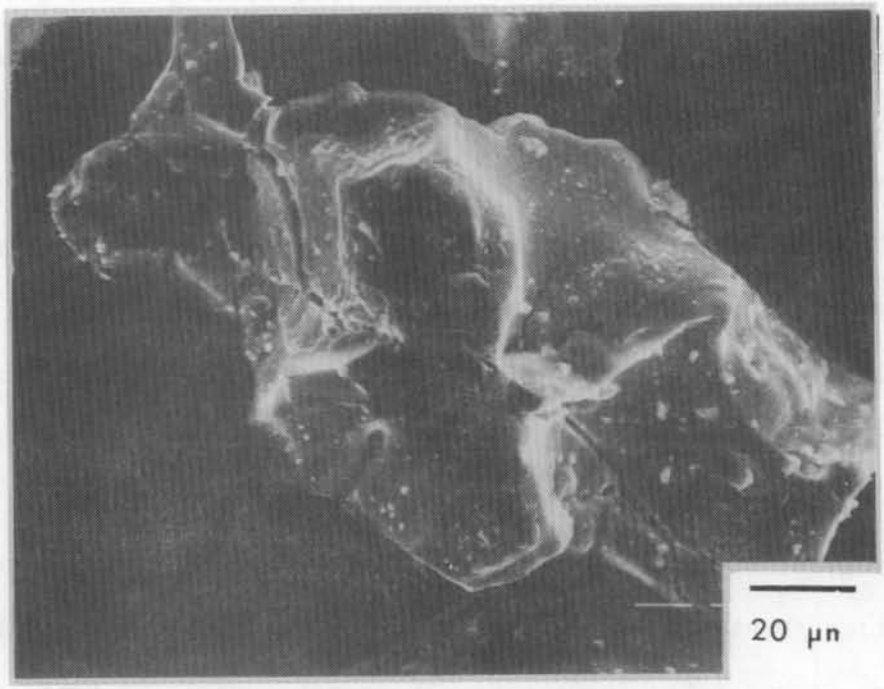

Figure 19 - Zirconia particle air quenched from 1200°C to room temperature.

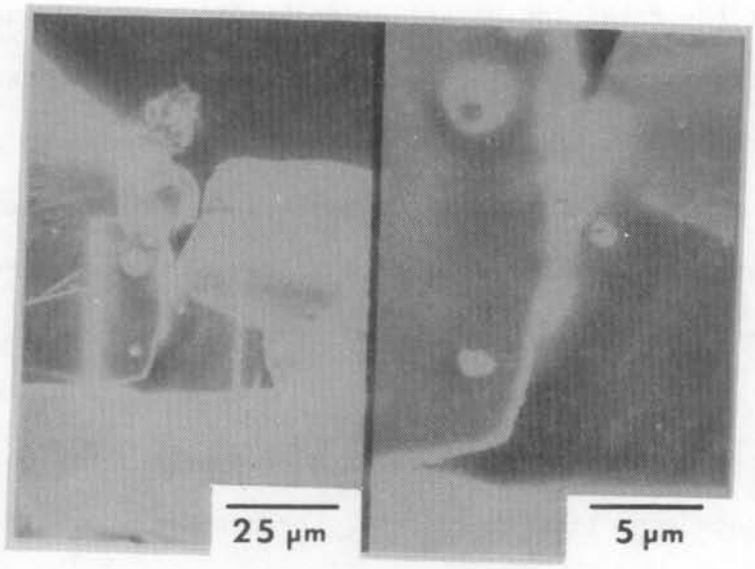

Figure 20 - Contact point between silicon carbide particles after heating at 1250°C for 24 hours in air

particle flow. Therefore, aggregation was examined as a function of time at temperature at 1000°C. As shown in Table 5, there is no increase in aggregation at 1000°C for times up to 24 hrs. with these materials.

Pressure enhances the driving force for material transport during sintering. Therefore, a pressure of 0.34 MPa (50 psi) was applied to the powders during heating at 1000°C. The rutile powder was adversely affected and showed no flowability after 1 hour (Table 6). The alumina powder also did not flow after 24 hours. Again, the aggregation of the alumina was very weak and it could be made to flow again by light agitation. However, in these experiments, if the powder did not flow from the crucible, it was noted "N.F." (Tables 4-6). Both the silica and zircon flowed easily from the crucible after the pressure experiment. All of the powders sintered to form strong particulate masses when heated to 1250°C. The sinter necks formed after heat treatment appear to be glassy in nature for the zircon, silica, rutile and silicon carbide (Figures 20-23), suggesting the presence of impurities which react to form low melting phases. Chemical analysis of the starting material corroborates this observation. The rutile and zircon particles contain significant amounts of free silica. The silica particles contain a significant quantity of potash (K_2O).

SUPPLEMENTAL STUDIES

To obtain a first order approximation of the effects of particle handling on particle attrition while in use at the Solar Receiver Facility, some simple milling experiments were performed. A cylindrical one gallon porcelain ball mill was filled approximately 1/4 full with powder that had been sized to +100 mesh (140 micrometers). After milling for 24 hours, the quantity less than 100 mesh was determined by sieving.

Table 4: Powder Flowability (cc/sec) After Heating for One Hour in Air

Temp (C.)	Material				
	Alumina-5	Rutile	Silicon carbide-2	Silica	Zircon
As-received	0.63	1.18	0.86	1.13	1.20
800	0.62	1.12	0.75	1.06	1.26
1000	0.66	1.15	N.F.	1.11	1.34
1100	0.63	1.18	N.F.	1.21	1.30
1200	N.F.	N.F.	N.F.	N.F.	1.26
1500	N.F.	N.F.	N.F.	N.F.	N.F.

N.F. = No Flow

Table 5: Powder Flowability (cc/sec) After Heating at 1000°C in Air

	Material			
	Alumina-5	Rutile	Silica	Zircon
Time (hrs.)				
As-received	0.63	1.18	1.13	1.20
4	0.6	1.24	1.20	1.34
8	0.65	1.21	1.18	1.34
12	0.68	1.21	1.20	1.34
24	0.67	1.18	1.18	1.30
24 at 1250°C	0.69	N.F.	0.51	1.13

N.F. = No Flow

Table 6: Powder Flowability (cc/sec) After Heating at 1000°C
0.34 MPa, In Air

	Material			
	Alumina-5	Rutile	Silica	Zircon
Time (hrs.)				
As-received	0.63	1.18	1.13	1.20
1	0.68	N.F.	1.26	1.34
4	0.68	N.F.	1.18	1.34
8	0.68	N.F.	1.19	1.34
12	0.68	N.F.	1.19	1.34
24	N.F.	N.F.	1.21	1.36
24 at 1250°C., 0.34 MPa	N.F.	N.F.	N.F.	N.F.

N.F. = No Flow

In the case of alumina-5, 1% of the material after milling was -100 mesh. However, Figure 24 indicates that the once sharp, irregular particles were reduced to fine equiaxed particles by milling. Although only a small amount of -100 mesh material was produced, previous studies have illustrated sinterability of this sub-population of particles is significantly enhanced relative to the coarse particles [13].

Interestingly, the aspect ratio of the rutile and zircon particles appeared to increase during milling; approximately 2% of the powders in each case was -100 mesh after milling.

Severe attrition of the silicon carbide occurred, yielding 93% of the particles as -100 mesh after milling. Figure 25 shows that cleavage of the crystallized silicon carbide is the major mechanism for particle size reduction.

SUMMARY AND RECOMMENDATIONS

Eight ceramic materials were evaluated as candidates for thermal transfer media for the High temperature Solid Particle Solid Receiver. Preliminary screening studies of particle flow and packing characteristics before and after heating to 1200°C were performed to reduce the number of materials to those deemed most likely to perform well under conditions of temperature, pressure, and storage time anticipated for receiver operation. Five materials were chosen for additional studies: alumina, zircon, silica, rutile, and silicon carbide. Each of these commercially obtained materials was classified to give 100 micrometer particles that were characterized with respect to sinterability. Sintering experiments were carried out from 1000°C to 1500°C for times of 1 to 24 hours. Samples were qualitatively analyzed for sintering between particles and the effect of aggregation due

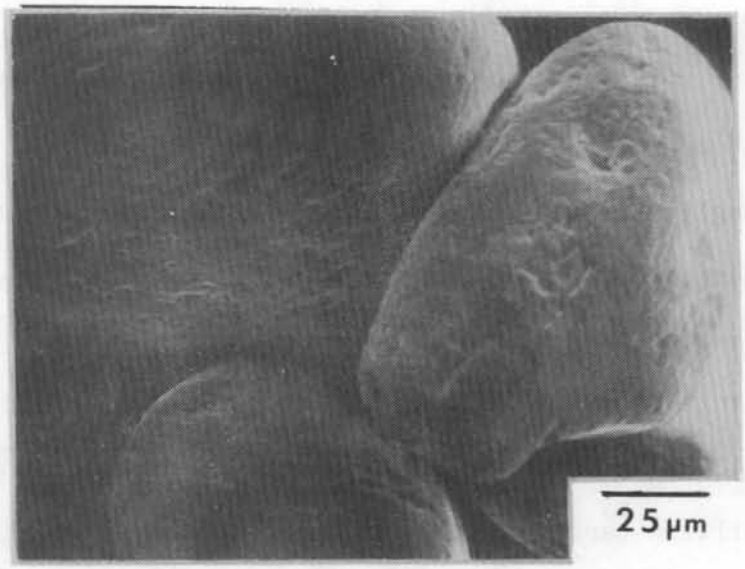

Figure 21 - Zircon particles heated at 1250°C., 0.34 MPa for 24 hours in air.

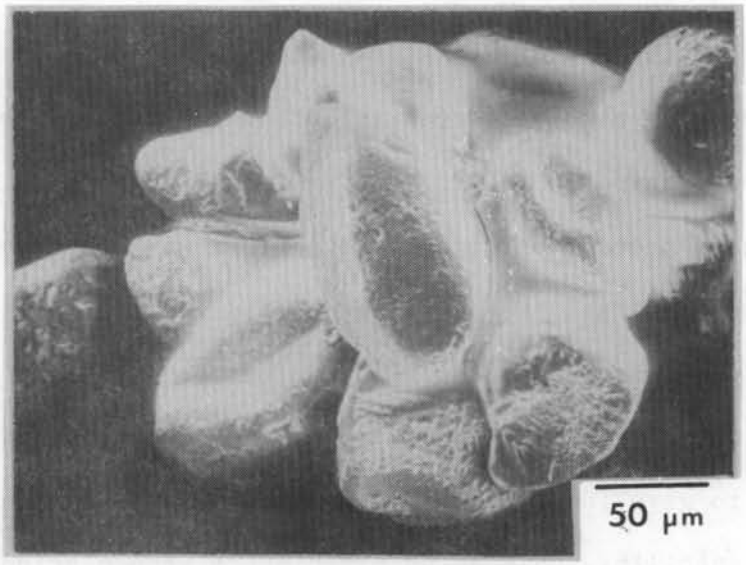

Figure 22 - Silica particles heated at 1250°C for 24 hours in air.

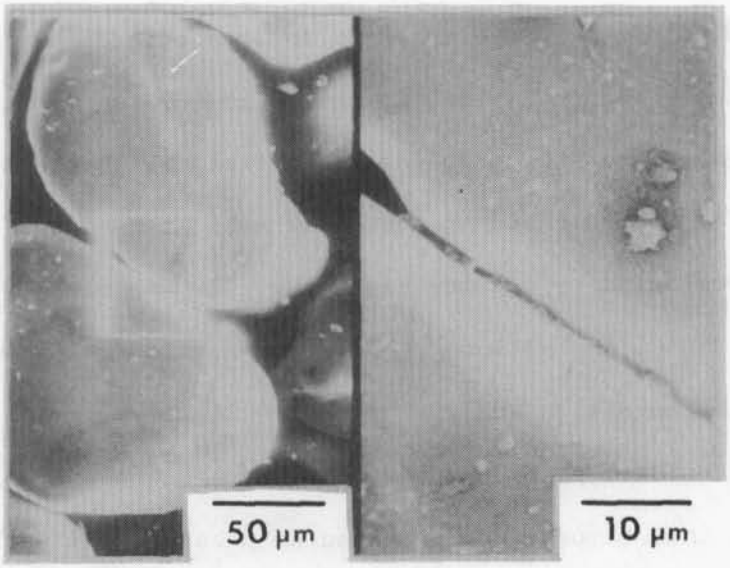

Figure 23 - Sinter necks between two rutile particles heated at 1250°C for 24 hours.

to sintering was judged by particle flowability. SEM studies were used to assess the nature of bond formation between particles that exhibited sintering.

The results of the above analyses are presented in summary form in Table 7. After 24 hours at 1000°C, the silica, zircon, rutile and alumina were unaggregated and showed no adverse effect due to the thermal treatment. Silicon carbide formed a strong, coherent mass as a result of extensive oxidation accompanied by viscous sintering. It was clearly shown that after 24 hours at 1250°C, the silicon carbide and rutile formed strong, sintered masses whereas the silica and zircon formed lightly aggregated masses that significantly reduced particle flowability. Alumina was essentially unaffected at this temperature provided no pressure was applied to the particle bed. The sintering in all cases was a result of a glassy phase formed during heating that yields a strong bond between particles. It was suggested that in most cases glass phase formation is enhanced by the presence of impurities in the commercially available materials. Pressure experiments at 1000°C showed that only the rutile and silicon carbide formed strongly sintered masses. However, at 1250°C and 0.34 MPa all materials sintered to form strong, coherent masses after 24 hours.

From these experiments, alumina and zircon are clearly the most desirable materials in terms of their high temperature stability. Rutile and silicon carbide are the worst materials as they both aggregate at 1000°C under pressure. Silica is intermediate in that it does not strongly aggregate at 1000°C but shows significant bond formation and aggregation at 1250°C.

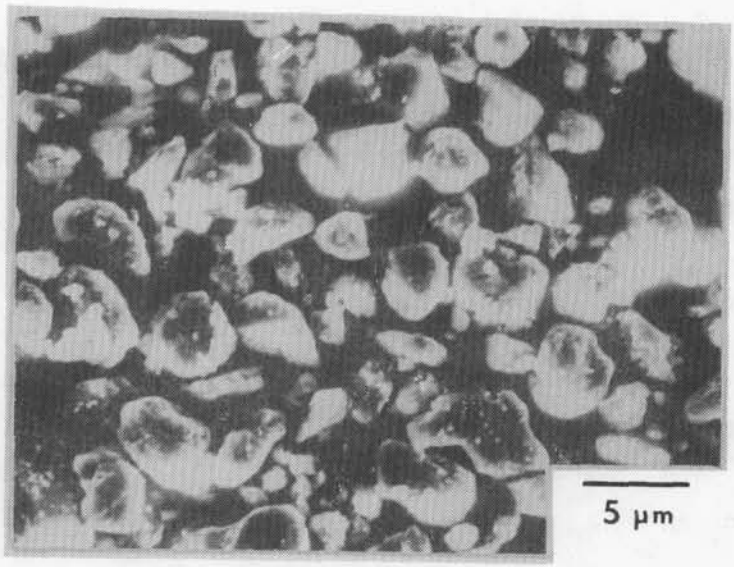

Figure 24 - Alumina-5 particles after milling for 24 hours

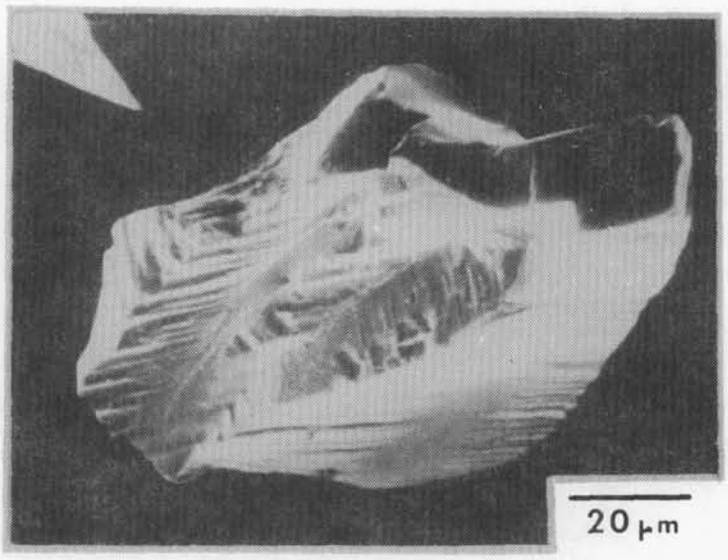

Figure 25 - Fracture surface of silicon carbide particle after milling for 24 hours.

Table 7: Summary of Aggregation Studies

Material	Aggregation (1000°C., 24 hrs., 0 MPa)	Aggregation (1000°C., 24 hrs., 0.34 MPa)	Aggregation (1250°C., 24 hrs., 0 MPa)	Aggregation (1250°C., 24 hrs., 0.34 MPa)	Attrition (24 hrs. % -100 mesh)
Alumina (Al_2O_3)	no	yes*	yes*	yes	1%
Silica (SiO_2)	no	no	yes	yes	1%
Silicon Carbide (SiC)	yes	yes	yes	yes	93%
Rutile (TiO_2)	no	yes	yes	yes	2%
Zircon	no	no	yes	yes	3%

* weak aggregation

FUTURE STUDIES

The behavior of the candidate materials as a function of temperature, pressure, and time was assessed for a narrow particle size distribution (nominally 100 μm). The sinterability and hence, flowability can be markedly affected by additions of finer particles. Generation of a sub-population of fines can be expected to occur during receiver operation due to wear, thermal shock, and impact induced fracture. The sinterability of a multimodal particle size distribution of zircon and alumina is currently being evaluated.

Although alumina and zircon both exhibit moderately low sinterability and may be acceptable candidates for thermal storage, both materials possess relatively low absorptivities in the solar spectrum [10]. Higher solar absorptivities may be required to heat the particles to the temperatures required for receiver operation. One method of enhancing absorptance is to dope the particles with impurities such as Fe, Ti, Mn, Cr, etc. However, dopants may significantly alter the sintering characteristics as well as increase the cost of the particles. We are currently evaluating the sinterability and strength characteristics of bauxite-based, refractory ceramic particles which possess solar absorptivities high enough to permit their use in the solar receiver.

REFERENCES

1. Battelson, K. W., "Solar Power Tower Design Guide: Solar Thermal Central Receiver Powder Systems, A Source of Electricity and/or Process Heat", SAND81-8005, April 1981.

2. Falcone, P. K., Noring, J. E., and Hackett, C. E., "Evaluation and Application of Solid Thermal Energy Carriers in High Temperature Solar Central Receiver System", Proceedings of the 17th IECEC, Los Angeles, CA, August 8-12, 1984.

3. Martin, J. and Vitko, J. Jr., "ASCUAS: A Solar Central Receiver Utilizing a Solid Thermal Carrier", SAND82-8203, January 1982.

4. Schmalfeld, "Le Four de Cracking Au Sable Lurgi-Rehrgas et Son Application A La Production D'Olefines", Chimie and Industrie - Science et Technique 86 (1961) 231.

5. Noring, J. E., Sandia National Laboratories, Livermore, private communication.

6. Barringer, E. A. and Bowen, H. K., "Formation, Packing, and Sintering of Monodisperse TiO_2 Powders," J. Am. Ceram. Soc., 65 (12) C-199 (1982).

7. Sacks, M. D. and Tseng, T. Y., "Preparation of SiO_2 from Model Powder Compacts: I, Formation and Characterization of Powders, Suspensions, and Green Compacts," J. Am. Ceram. Soc., 67 (8) 526-532 (1984).

8. Rhines, F. N., "Dynamic Particle Stacking," in Ceramic Processing Before Firing, ed. by G. Y. Onoda, Jr. and L. L. Hench, John Wiley & Sons, New York, (1978) pp. 321-341.

9. Hinze, J. W. and Graham, H. C., "The Active Oxidation of Si and SiC in the Viscous Gas-Flow Regime," Electrochem. Soc., 123, 1066-1078 (1976).

10. Pettit, R. B. and Mahoney, A. R., internal memorandum "Optical Properties of Ceramic Particles," dated September 1, 1983.

11. Hruby, J. M., Steele, B. R., and Burolla, V. P., "Solid Particle Receiver Experiments: Radiant Heat Test," SAND84-8251.

12. Singhal, S. C., "Oxidation Kinetics of Hot-Pressed Silicon Carbide," J. Mater. Sci., 11, 1246-1253 (1976).

13. Messing, G. L. and Onoda, G. Y., "The Sintering of Inhomogeneous Binary Powder Mixtures," J. Am. Ceram. Soc., 64 (8) 468-72 (1981).

Appendix: Vendor's Chemical Analysis

Material	Typical Chemical Analysis (w/o)	
Alumina-1 (Norton)	Al_2O_3	99.55
	TiO_2	0.01
	SiO_2	0.05
	Fe_2O_3	0.04
	CaO	0.03
	MgO	0.02
	Alkali	0.30
Alumina-2 (Carborundum)	Al_2O_3	99.53
	SiO_2	0.04
	Fe_2O_3	0.10
	Na_2O	0.33
Alumina-3 (Washington Mills)	Al_2O_3	99.53
	Na_2O	0.14
	Fe_2O_3	0.08
	SiO_2	0.03
	CaO	0.03
	TiO_2	0.01
	C	0.0034
	S	0.0015
Alumina-5 (Kaiser)	Al_2O_3	99.8
	Alpha phase	99.3
	SiO_2	0.06
	Fe_2O_3	0.03
	Na_2O	0.03
Alumina-7 (General Abrasives)	Al_2O_3	>90
	SiO_2	1-4
	TiO_2	2-5
	B	0.002
	Mn	0.03
	Fe	0.1
	Mg	0.2
	Cr	0.02
	Ca	0.05
	Zr	0.1
	Sr	0.004
Silicon carbide-1 (Norton)	SiC	98.06
	Si	0.63
	SiO_2	0.57
	C	0.25
	Fe	0.16
	Al	0.23
	Ca	0.05
	Mg	0.05

Silicon carbide-2 (Carborundum)	SiC	97.0
	SiO_2	0.6
	Si	0.8
	Fe	0.2
	Al	0.3
	Ca	0.6
Silicon carbide-3 (Washington Mills)	SiC	98.5
	Si	0.5
	SiO_2	0.5
	C	0.3
	Fe	0.1
	Al	0.2
Silicon carbide-5 (General Abrasives)	SiC	97.05
	C (free)	0.66
	C (total)	29.73
Garnet- (Cont. Min. Proc.)	Staurolite	77
	Tourmaline	10
	Titanium minerals	4
	Kyanite	2
	Zircon	3
	Quartz	4
Rutile- (Cont. Min. Proc.)	TiO_2	96.70
	Fe_2O_3	0.55
	ZrO_2	1.00
	SiO_2	0.48
	S	0.01
	Al_2O_3	0.16
	CaO	0.06
	MgO	0.02
Silica- (Unimin Corp.)	SiO_2	>98
	Al_2O_3	0.73
	K_2O	0.63
	B	0.005
	Mn	0.005
	Fe	0.08
	Mg	0.04
	Ti	0.04
	Ca	0.03
	Cu	0.003
	Zr	0.05
	Na	0.01
	Sr	0.003

Zircon- (Cont. Min. Proc.)	ZrO_2	65.50
	SiO_2	33.50
	TiO_2	0.25
	SiO_2 (free)	0.12
	Fe_2O_3	0.04
	Al_2O_3	1.70
Mullite- (C.E. Minerals)	Al_2O_3	76.4
	SiO_2	23.0
	K_2O	0.04
	Na_2O	0.29
	MgO	0.11
	CaO	0.09
	TiO_2	0.03
	Fe_2O_3	0.05
Zirconia- (Norton)	$ZrO_2 + HfO_2$	94.45
	HfO_2	2.0
	CaO	4.50
	SiO_2	0.30
	TiO_2	0.05
	Fe_2O_3	0.15
	Al_2O_3	0.65

DISTRIBUTION:

Dr. W. E. Brown
Director of Technology
Norton-Alcoa Proppants
12221 Merit Dr.
Suite 1040
Dallas, TX 75251-2216

Dr. G. L. Messing (2)
Department of Materials
Science and Engineering
The Pennsylvania State University
University Park, PA 16802

Dr. R. C. Bradt
Chairman
Department of Materials
Science and Engineering
Roberts Hall FB-10
Seattle, WA 98195

U.S. Department of Energy (5)
Forrestal Building, Room 5H021
Code CE-314
1000 Independence Avenue, S.W.
Washington, D.C. 20585
Attn: C. Carwile
H. Coleman
C. Mangold
F. Morse
M. Scheve

U.S. Department of Energy(2)
P. O. Box 5400
Albuquerque, NM 87115
Attn: D. Graves
J. Weisiger

U.S. Department of Energy(2)
1333 Broadway
Oakland, CA 94612
Attn: T. Vaeth
R. Hughey

Washington State University
Department of Mechanical Engineering
Pullmann, WA 99164-2920
Attn: Prof. C. Crowe

Center for Materials Science
Inorganic Materials Division
National Bureau of Standards
Washington, D.C. 20234
Attn: S. M. Wiederhorn

Centre National Da La Recherche Scientifique(2)
Laboratorie d'Energetique Solaire
Odiello, B.P. 5, 66120 Font-Romeu
France
Attn: G. Flamant
C. Foyere

Electric Powder Research Institute(2)
P. O. Box 10412
Palo Alto, CA 94303
Attn: J. Bigger
E. Demeo

Electro-Optic Systems Section
Pacific Northwest Laboratories
Battelle Boulevard
Richland, WA 99352
Attn: J. W. Griffin

Solar Energy Research Institute (4)
1617 Cole Boulevard
Golden, CO 80401
Attn: M. Carasso
R. Copeland
B. Gupta
H. Hulstram

Lawrence Berkeley Laboratories 90-2024
Berkeley, CA 94720
Attn: A. Hunt

Lawrence Livermore National Laboratory, L-200
Attn: O. R. Walton

Quartz Products Corporation
P.O. Box 1347
688 Somerset Street
Plainview, NJ 07061
Attn: Mr. Jacques Mercier

Dresser Industries, Inc.
General Abrasive Division
Route 5
Box 58
Eufala, AL 36027-9501
Attn: Mr. Tom C. Palamara
Manager, Process Engineering

1800 R. L. Schwoebel
1820 R. E. Whan
1824 J. N. Sweet
1824 R. A. Mahoney
1824 R. B. Pettit
1840 R. J. Eagan (2)
1842 R. E. Loehman
1842 J. R. Hellmann (5)
1845 T. A. Michalske
1846 D. H. Doughty
3141-1 C. M. Ostrander (5)
4031 Patents
6000 E. H. Beckner, Attn: V. Dugan, 6200
7476 R. H. Moore
8313 R. W. Bradshaw
8400 R. C. Wayne
8450 J. B. Wright
8473 J. C. Swearengen
8471 P. K. Falcone
8473 J. M. Hruby
8446 B. R. Steele